Manganese(II) Complexes containing the Tridentate Ligands 2,6-Bis[1-(phenylimino)ethyl]pyridine, L^1, or 2,6-Bis[1-(4-methoxyphenylimino)ethyl]pyridine, L^2. The Molecular Structures of Five-co-ordinate $[MnBr_2L^1]$ and the Zinc Analogue $[ZnCl_2L^1]$†

Dennis A. Edwards,* Mary F. Mahon, William R. Martin, and Kieran C. Molloy
School of Chemistry, University of Bath, Bath BA2 7AY
Phillip E. Fanwick and Richard A. Walton
Department of Chemistry, Purdue University, West Lafayette, Indiana 47907, U.S.A.

Reactions of equimolar ratios of $MnX_2·4H_2O$ (X = Cl or Br) and the tridentate ligands 2,6-bis[1-(phenylimino)ethyl]pyridine (L^1) or 2,6-bis[1-(4-methoxyphenylimino)ethyl]pyridine (L^2) afford the five-co-ordinate complexes $[MnX_2L^1]$ and $[MnX_2L^2]$. The complex $[MnBr_2L^1]$, as the monobenzene solvate, crystallises in the space group $P2_12_12_1$ with a = 8.761(3), b = 17.032(5), c = 17.453(5) Å, and Z = 4. The distorted trigonal-bipyramidal geometry around manganese involves a trigonal plane with angles close to 120° comprising both bromines and the pyridyl nitrogen of L^1. However, strain induced by this ligand reduces the axial NMnN angle to 142.8°. The Mn–N(pyridyl) bond is markedly shorter than the axial Mn–N(imino) bonds. For comparison, the structure of $[ZnCl_2L^1]$, as the 1.5MeCN solvate, has been determined. This complex crystallises in the triclinic space group $P\bar{1}$ with a = 8.977(3), b = 12.585(5), c = 22.297(6), α = 90.99(3), β = 98.27(2), γ = 94.33(3)°, and Z = 4. The two independent molecules of $[ZnCl_2L^1]$ in the asymmetric unit are geometrically identical within the limits of experimental error, with bond lengths and angles differing by less than twice the estimated standard deviations. The distorted trigonal-bipyramidal geometry and bond length and angle variations are similar to those of the manganese complex. Reactions of $Mn(ClO_4)_2·6H_2O$ with 2 equivalents of L^1 or L^2 produce the cations $[MnL^1_2]^{2+}$ and $[MnL^2_2]^{2+}$ isolated as the perchlorates. The two ligands of the octahedral cations are co-ordinated in a meridional manner.

The donor properties of ligands of type L have received some attention in recent years. They normally behave as planar tridentate ligands, for example, in reactions with nickel(II), copper(II), zinc and cadmium halides, nitrates, perchlorates, and tetrafluoroborates.[1–8] The products of these reactions were proposed to be either five-co-ordinate $[MX_2L]$ complexes or six-co-ordinate species such as $[ML_2]^{2+}$, $[M(\eta^2\text{-}NO_3)X(L)]$, $[M(\eta^2\text{-}NO_3)(NO_3)L]$, or $[M(NO_3)(en)L]^+$ (M = Ni, Cu, Zn, or Cd; X = halide; en = 1,2-diaminoethane; not all combinations). Few of these complexes have been structurally characterised, the only single-crystal *X*-ray structure determinations being of $[M(\eta^2\text{-}NO_3)(NO_3)L^1]$ (M = Ni[2,3] and Cu[4]), $[NiL^3_2][BF_4]_2$,[8] and $[Cu(bipy)L^4(FBF_3)][BF_4]$ (bipy = 2,2′-bipyridine).[9] Recently, a further type of behaviour has been recognised[10,11] in that L^1 and L^5 react with Group 6 and 7 metal carbonyls or derivatives to yield complexes in which the potentially tridentate ligands act in a bidentate chelating mode, binding to the metal centre *via* the pyridyl nitrogen and just one of the imino nitrogen atoms. This co-ordination type has been confirmed by a single-crystal *X*-ray structure determination[10] of *cis*-$[Mo(CO)_4L^5]$.

We describe here the syntheses of some five- and six-co-ordinate manganese(II) complexes containing L^1 or L^2 and report the full structural characterisation of $[MnBr_2L^1]$ and the known[1] zinc analogue $[ZnCl_2L^1]$. These are the first five-co-ordinate complexes containing ligands of type L to be studied by single-crystal *X*-ray crystallography. The only related studies of manganese(II) complexes[12,13] concern the use of the dioxime ligand L^6. Supposed five-co-ordinate $[MnX_2L^6]$ and six-co-ordinate $[MnL^6_2]X_2$ (X = halide, NO_3, NCS, or NCSe) were isolated.[12] However, subsequent studies[13] showed conclusively that in the solid state $[MnCl_2L^6]$ is an infinite polymer with pentagonal-bipyramidal co-ordination of each manganese centre being achieved by bridging chloride ligands occupying axial and equatorial sites on adjacent monomer units in the helical chains. Evidence obtained from e.p.r. spectroscopy suggests that in dimethylformamide solution the polymer breaks down to give either dimeric or tetrameric $[\{MnCl_2L^6\}_n]$

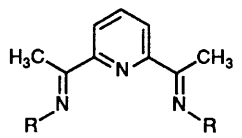

L

	R
L^1	Ph
L^2	C_6H_4OMe-4
L^3	$(CH_2)_3Ph$
L^4	C_6H_4Et-4
L^5	CH_2CMe_3
L^6	OH

† {2,6-Bis[1-(phenylimino-κ*N*)ethyl]pyridine-κ*N*}dibromomanganese(II) and {2,6-Bis[1-(phenylimino-κ*N*)ethyl]pyridine-κ*N*}-dichlorozinc(II).

Supplementary data available: see Instructions for Authors, *J. Chem. Soc., Dalton Trans.*, 1990, Issue 1, pp. xix—xxii.

Non-S.I. units employed: eV ≈ 1.60 × 10^{-19} J, G = 10^{-4} T.

(n = 2 or 4) complexes. In the light of this work, we wished to establish the structural nature of the proposed five-co-ordinate $[MnX_2L^1]$ and $[MnX_2L^2]$ (X = Cl or Br) complexes reported here, so the structure of $[MnBr_2L^1]$ was determined. Apart from a five-co-ordinate monomeric formulation, other possibilities include a six-co-ordinate dimer $[(L^1)BrMn(\mu\text{-}Br)_2MnBr(L^1)]$, a six-co-ordinate cubane-type tetramer $[\{MnBr(\mu_3\text{-}Br)L^1\}_4]$, or a seven-co-ordinate polymer $[\{Mn(\mu\text{-}Br)_2L^1\}_\infty]$.

Experimental

Starting Materials.—The ligands 2,6-bis[1-(phenylimino)-ethyl]pyridine (L^1) and 2,6-bis[1-(4-methoxyphenylimino)-ethyl]pyridine (L^2) were prepared as previously described.[1] Their purity was confirmed by m.p. determinations, elemental microanalyses, mass and n.m.r. spectra. Compound L^1: yield 89%; m.p. 159 °C (lit.,[1] 157—158 °C); mass spectrum, *m/z* 313, (M^+), 298, 220, 118, and 77; ^{1}H n.m.r. ($CDCl_3$, 270 MHz), δ 8.40 (d, py, 2 H), 7.85 (t, py, 1 H), 7.40 (t, Ph, 4 H), 7.15 (t, Ph, 2 H), 6.90 (d, Ph, 4 H), and 2.42 (s, CH_3, 6 H); ^{13}C n.m.r. ($CDCl_3$, 67.8 MHz), δ 167.2, 155.5, 151.4, 136.7, 128.9, 124.7, 122.3, 118.0, and 16.1 p.p.m. (Found: C, 80.5; H, 6.10; N, 13.4. Calc. for $C_{21}H_{19}N_3$: C, 80.5; H, 6.10; N, 13.4%). Compound L^2: yield 72%; m.p. 190 °C (lit.,[1] 190—192 °C); mass spectrum, *m/z* 373 (M^+), and 148; ^{1}H n.m.r. ($CDCl_3$, 270 MHz), δ 8.34 (d, py, 2 H), 7.84 (t, py, 1 H), 6.92—6.83 (m, 4-$MeOC_6H_4$, 8 H), 3.83 (s, MeO, 6 H), and 2.42 (s, CH_3, 6 H); ^{13}C n.m.r. ($CDCl_3$, 67.8 MHz), δ 167.4, 156.2, 155.6, 144.3, 136.7, 122.0, 120.8, 114.2, 55.4, and 16.1 p.p.m. (Found: C, 74.1; H, 6.20; N, 11.3. Calc. for $C_{23}H_{23}N_3O_2$: C, 74.0; H, 6.20; N, 11.3%).

The zinc complex $[ZnCl_2L^1]$ was isolated from the reaction of L^1 (1.28 g) with a mixture of $Zn(NO_3)_2\cdot 6H_2O$ (1.22 g) and NaCl (0.77 g) in refluxing aqueous ethanol (10 cm^3 water and 100 cm^3 EtOH). Yield 94%. ^{1}H N.m.r. (CD_2Cl_2, 270 MHz): δ 8.40—7.00 (m, py + Ph, 13 H) and 2.55 (s, CH_3, 6 H) (Found: C, 56.1; H, 4.20; N, 9.35. Calc. for $C_{21}H_{19}Cl_2N_3Zn$: C, 56.1; H, 4.25; N, 9.35%).

Synthesis of Manganese(II) Complexes.—(*a*) $[MnX_2L^1]$ *and* $[MnX_2L^2]$ (X = Cl *or* Br). The preparation of these complexes is based upon the same general procedure. A quantity of $MnX_2\cdot 4H_2O$ (*ca.* 1 g) was dissolved in 95% ethanol (50 cm^3) and 1 molar equivalent of L^1 or L^2 added. The reaction mixture was brought to reflux for up to 1 h and then cooled to 0 °C. The insoluble reaction product, often obtained after reduction of the volume of solvent, was filtered off, washed or recrystallised, and finally dried *in vacuo*.

(*i*) $[MnCl_2L^1]$. Pale orange solid; washed with ethanol and chloroform. Yield 81% (Found: C, 57.5; H, 4.40; N, 9.60. Calc. for $C_{21}H_{19}Cl_2MnN_3$: C, 57.4; H, 4.35; N, 9.55%).

(*ii*) $[MnBr_2L^1]$. Pale orange solid; recrystallised from ethanol. Yield 84% (Found: C, 47.6; H, 3.75; N, 7.85. Calc. for $C_{21}H_{19}Br_2MnN_3$: C, 47.8; H, 3.65; N, 7.95%).

(*iii*) $[MnCl_2L^2]$. Orange solid; washed with ethanol and diethyl ether. Yield 71% (Found: C, 55.6; H, 4.70; N, 8.50. Calc. for $C_{23}H_{23}Cl_2MnN_3O_2$: C, 55.3; H, 4.65; N, 8.40%).

(*iv*) $[MnBr_2L^2]$. Rust-brown solid; recrystallised from ethanol in the presence of a little $MnBr_2\cdot 4H_2O$. Yield 77% (Found: C, 46.7; H, 3.75; N, 7.10. Calc. for $C_{23}H_{23}Br_2MnN_3O_2$: C, 47.0; H, 3.95; N, 7.15%).

(*b*) $[MnL^1{}_2][ClO_4]_2$ *and* $[MnL^2{}_2][ClO_4]_2$. These complexes were prepared by mixing $Mn(ClO_4)_2\cdot 6H_2O$ with L^1 or L^2 in 1:2 molar equivalents in 95% ethanol, heating the mixture to reflux, followed by work-up as described in (*a*).

(*i*) $[MnL^1{}_2][ClO_4]_2$. Dark orange solid; washed with ethanol and water. Yield 91% (Found: C, 56.2; H, 4.30; N, 9.50. Calc. for $C_{42}H_{38}Cl_2MnN_6O_8$: C, 57.3; H, 4.35; N, 9.55%).

(*ii*) $[MnL^2{}_2][ClO_4]_2$. Dark brown solid; recrystallised from ethanol. Yield 94% (Found: C, 55.8; H, 4.50; N, 8.50. Calc. for $C_{46}H_{46}Cl_2MnN_6O_{12}$: C, 55.2; H, 4.65; N, 8.40%).

Preparation of Single Crystals of $[MnBr_2L^1]$ *and* $[ZnCl_2L^1]$.—Crystals of $[MnBr_2L^1]$ suitable for *X*-ray crystallographic studies were obtained by layering benzene over an acetone solution of the complex. The small orange crystals that grew were found to be those of a monobenzene solvate. Single crystals of the zinc complex $[ZnCl_2L^1]$ were grown from acetonitrile. These crystals were shown to have the stoicheiometry $[ZnCl_2L^1]\cdot 1.5MeCN$ (Found: C, 56.6; H, 4.65; N, 12.0. Calc. for $C_{24}H_{23.5}Cl_2N_{4.5}Zn$: C, 56.4; H, 4.65; N, 12.3%).

X-Ray Crystal Structure Analyses.—$[MnBr_2L^1]$. Cell parameters were based upon 25 reflections in the range $13 < \theta < 17°$. Three standard reflections were measured every 5 000 s of beam exposure and displayed no systematic variation. Data were corrected for Lorentz, polarisation and absorption effects, but not extinction. A full listing of crystal data and experimental variables is given in Table 1.

The structure was solved by standard Patterson and Fourier techniques. All atoms were refined anisotropically except those carbons of the lattice benzene molecule and corrections for anomalous scattering applied.[14] Hydrogen atoms were included at calculated positions (C–H 95 pm) assuming ideal geometry. For the methyl groups, one hydrogen was located in a Fourier difference map, its position idealised, and the remaining positions calculated. For these hydrogens the values of the isotropic thermal parameters were taken as $B(H) = 1.3B_{equiv.}(C)$ at the time of their inclusion in the refinement procedure. Hydrogen atoms were not included in the least-squares refinement, but were included in the calculation of $F_{calc.}$. Since the space group $P2_12_12_1$ is enantiomorphic, refinement was performed on both orientations without the inclusion of hydrogen atoms. The final residuals for the two enantiomorphs were as follows: $R = 0.046$ and $R' = 0.050$; $R = 0.056$, and $R' = 0.063$. Refinement was continued with the enantiomer with the lower R factor until covergence was met. The final Fourier difference map showed a maximum peak of 0.84e Å^{-3} of no chemical significance. The least-squares program minimised the function $\Sigma\, w(|F_o| - |F_c|)^2$, where w is a weighting factor defined as $w = [\sigma^2(F_o)]^{-1}$.

An ORTEP representation of the asymmetric unit, with atomic labelling, is shown in Figure 1. Final atomic co-ordinates and intramolecular bond distances and angles are given in Tables 2 and 3.

$[ZnCl_2L^1]$. Cell parameters were based upon 12 reflections in the range $13 < \theta < 17°$. A monitor reflection, measured after every 50 reflections, showed no systematic variation. Data were corrected for Lorentz and polarisation but not absorption effects. A full listing of crystal data and experimental variables is given in Table 1.

The structure was solved by direct methods and Fourier difference techniques. The asymmetric unit consists of two independent molecules of the zinc complex, along with three molecules of acetonitrile solvate. Refinement was blocked matrix, with each independent molecule making up a block, the solvent molecules being treated separately as a third block. The zinc, chlorine, and nitrogen atoms along with the atoms of the solvate molecules were refined anisotropically, all other atoms isotropically. Hydrogen atoms were included at calculated positions with fixed U_{iso} values (0.05 Å^2). The final difference map showed its maximum and minimum features at 0.24 and −0.22e Å^{-3} respectively. In the final cycles of refinement a weighting scheme of the form $w = 4.2969\,[\sigma^2(F_o) + 0.000\,131\,F_o{}^2]^{-1}$ was used.

An ORTEP diagram showing the asymmetric unit, with labelling, is given in Figure 2. Final positional parameters

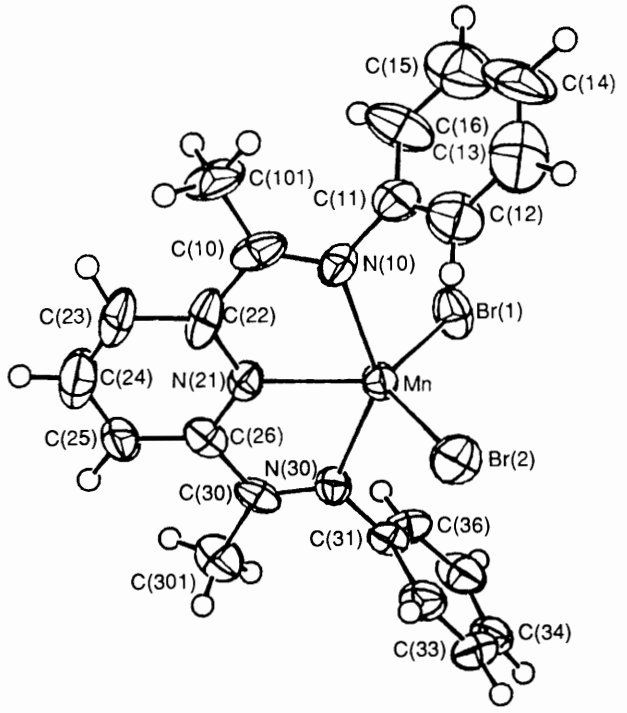

Figure 1. Structure of $[MnBr_2L^1]$ with the numbering scheme used

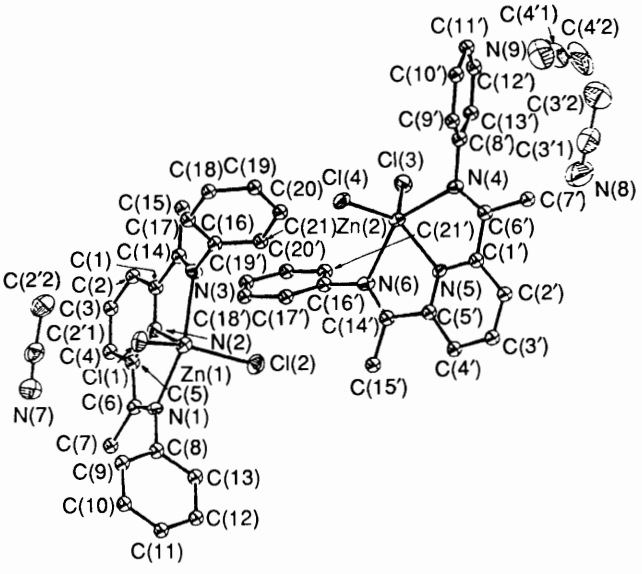

Figure 2. Structure of $[ZnCl_2L^1]$ showing both molecules and the three solvate molecules in the asymmetric unit with the numbering scheme used

and bond distances and angles are given in Tables 4 and 5 respectively. The atomic scattering factors and anomalous dispersion correction factors were taken from the usual literature sources.[15–18]

Additional material for both structures available from the Cambridge Crystallographic Data Centre comprises H-atom co-ordinates, thermal parameters, and remaining bond distances and angles.

Physical Measurements.—Infrared spectra were recorded over the ranges 4 000—600 and 600—200 cm^{-1} using Perkin-Elmer 1310 and 597 spectrophotometers, respectively. Samples were examined as Nujol mulls between NaCl and CsI plates over these frequency ranges. Molar conductivities were determined using a Wayne-Kerr Autobalance universal bridge and a dip-type cell with platinum electrodes. The *X*-band e.p.r. spectra of solid samples were measured at room temperature using a Varian E-3 spectrometer with diphenylpicrylhydrazyl as calibrant. Magnetic moment determinations were carried out by the Gouy method, using $[Ni(en)_3]S_2O_3$ as calibrant. Carbon, hydrogen, and nitrogen microanalyses were performed using a Carlo Erba elemental analyser. Proton and ^{13}C n.m.r. spectra were recorded in $CDCl_3$ or CD_2Cl_2 solutions using a JEOL GX 270 spectrometer. Mass spectra were obtained at ionisation energies 70 and 12 eV using a VG 7070E spectrometer.

Results and Discussion

The potentially tridentate ligands L^1 and L^2, prepared by condensation of 2,6-diacetylpyridine with 2 molar equivalents of the appropriate primary amine, have been treated in 95% ethanol with hydrated manganese(II) chloride, bromide, and perchlorate. Reactions of equimolar proportions of ligand and manganese(II) halide afford the complexes $[MnX_2L^1]$ and $[MnX_2L^2]$ (X = Cl or Br) whereas reactions of 2 molar equivalents of the ligands with 1 molar equivalent of $Mn(ClO_4)_2 \cdot 6H_2O$ produce the bis(ligand) complex cations $[ML^1_2]^{2+}$ and $[ML^2_2]^{2+}$, isolated as the ClO_4^- salts. All products had satisfactory C, H, and N elemental microanalyses.

(*a*) $[MnX_2L^1]$ *and* $[MnX_2(L^2)]$.—These complexes are stable in air at room temperature and insoluble in water and some characterisation data are listed in Table 6. Conductivities of 10^{-3} mol dm^{-3} solutions of the complexes in acetonitrile at 25 °C are in the range 30—60 S m^2 mol^{-1}, well below those displayed by 1:1 electrolytes in this solvent ($\approx$140 S m^2 mol^{-1}). The room-temperature magnetic moments are typical of high-spin d^5 manganese(II) complexes, $\mu_{eff.}$ values being in the range 5.8—5.9 ($\pm$0.1). The i.r. spectra between 4 000 and 600 cm^{-1} are not particularly informative, merely indicating that the ligands have co-ordinated intact to the metal centre, *i.e.* no ν(NH) or ν(C=O) bands are observed and the ligand bands *e.g.* ν(C=N) show only minor shifts on co-ordination. The low-frequency i.r. spectrum of each complex contains two bands that can be assigned to ν(Mn–X) vibrations ($A_1 + B_1$ for C_{2v} symmetry). The band positions are very similar to those of $[ZnCl_2L^1]$ [ν(Zn–Cl) 314s and 285ms] and the five-co-ordinate complexes[19] $[MnCl_2(paphy)]$ [ν(Mn–Cl) 300s and 280s (sh)] and $[MnBr_2(paphy)]$ [ν(Mn–Br) 247s and 226s (sh)] (paphy = *E*-pyridine-2-carbaldehyde 2′-pyridylhydrazone).

The *X*-band e.p.r. spectra of the four manganese complexes at room temperature merely consist of a single, broad, featureless resonance centred at $\approx$3 400 G ($g \approx 2$). However, a coprecipitated sample of $[MnCl_2L^1]$ in $[ZnCl_2L^1]$ at 5% dilution gives a well resolved room-temperature e.p.r. spectrum with intense resonances centred at 1 490 and 1 800 G each showing ^{55}Mn hyperfine structure and a much weaker, poorly resolved, signal centred at 3 400 G. The hyperfine coupling constant ($A \approx 77$ G) and the hyperfine intensity patterns are typical of a monomeric manganese(II) complex. This type of spectrum has previously been observed[20] for manganese(II) doped into the five-co-ordinate complex $[Zn\{N(CH_2CH_2NMe_2)_3\}I]I$ where the manganese ion site was assumed to be axial. The theoretical approach of Dowsing and Gibson[21] indicates that the rhombic zero-field splitting parameter *E* will be very close to zero and the axial zero-field splitting parameter *D* around 0.2 cm^{-1}.

The above data provide evidence favouring mononuclear five-co-ordination for the halide complexes and in order firmly to establish this and to determine the stereochemistry we have

Table 1. Crystal data and data collection parameters[a]

Formula	$C_{27}H_{25}Br_2MnN_3$	$C_{21}H_{19}Cl_2N_3Zn\cdot1.5CH_3CN$
M	606.28	511.235
Space group	$P2_12_12_1$	$P\bar{1}$
a/Å	8.761(3)	8.977(3)
b/Å	17.032(5)	12.585(5)
c/Å	17.453(5)	22.297(6)
α/°	90	90.99(3)
β/°	90	98.27(2)
γ/°	90	94.33(3)
U/Å^3	2 604.2	2 484.6
D_c/g cm^{-3}	1.546	1.367
Crystal dimensions/mm	0.50 × 0.24 × 0.14	0.35 × 0.25 × 0.25
μ cm^{-1}	35.46	11.53
F(000)	1 212.0	919.9
Absorption correction	Empirical[b]	
Transmission factors	0.63, 1.00	
Diffractometer	Enraf-Nonius CAD4	Hilger and Watts Y290
h,k,l limits	0—9, 0—18, 0—18	0—9, −13 to 13, −23 to 23
2θ range/°	4—45	4—44
Scan width/°	1.00 tan θ	
Take-off angle/°	1.90	
Programs used	Enraf-Nonius SDP	SHELX 86, SHELX 76, ORTEP
Data collected	1 974	5 635
Unique data	1 974	4 800
$I > 3\sigma(I)$	1 277	3 665
No. variables	268	[c]
Max. shift/e.s.d.	0.17	0.01
R	0.046	0.069
R'	0.050	0.065
Goodness of fit	1.362	

[a] Details in common: $Z = 4$; 20 °C; Mo-K_α radiation (λ = 0.710 69 Å); graphite monochromator; scan method ω—2θ. [b] Ref. 14. [c] 134 per block for each of the 2 $[ZnCl_2L^1]$ units and 81 for the block containing 3 MeCN units.

Table 2. Final fractional atomic co-ordinates for $[MnBr_2L^1]\cdot C_6H_6$

Atom	x	y	z	Atom	x	y	z
Mn	0.963 3(2)	0.667 6(1)	0.285 1(1)	C(26)	0.859(2)	0.810 3(8)	0.380 0(7)
Br(1)	0.778 7(2)	0.609 71(9)	0.194 77(9)	C(30)	0.790(2)	0.743 4(8)	0.419 2(7)
Br(2)	1.169 8(2)	0.587 09(9)	0.343 6(1)	C(31)	0.748(1)	0.605 6(7)	0.425 3(7)
N(10)	1.093(1)	0.741 1(5)	0.198 8(6)	C(32)	0.831(2)	0.559 8(8)	0.474 8(8)
N(21)	0.941(1)	0.790 1(5)	0.318 9(6)	C(33)	0.769(2)	0.492 9(9)	0.507 4(8)
N(30)	0.817(1)	0.675 9(5)	0.390 5(6)	C(34)	0.623(2)	0.471 3(8)	0.488 1(8)
C(10)	1.094(2)	0.815 6(8)	0.207 7(8)	C(35)	0.540(2)	0.514 0(9)	0.436 4(8)
C(11)	1.156(2)	0.707 9(8)	0.129 8(8)	C(36)	0.602(2)	0.583 6(8)	0.406 8(8)
C(12)	1.274(2)	0.665(1)	0.138 4(9)	C(101)	1.171(2)	0.875 0(8)	0.159 0(9)
C(13)	1.333(2)	0.618(1)	0.072(1)	C(301)	0.687(2)	0.760(1)	0.487 8(9)
C(14)	1.276(2)	0.635(1)	0.001 9(9)	C(401)	0.474(2)	0.437(1)	0.227(1)
C(15)	1.159(3)	0.686(1)	−0.003(1)	C(402)	0.385(2)	0.389(1)	0.275(1)
C(16)	1.097(2)	0.722(1)	0.059 3(8)	C(403)	0.397(2)	0.310(1)	0.270(1)
C(22)	1.014(2)	0.845 8(7)	0.276 1(8)	C(404)	0.503(2)	0.279(1)	0.221(1)
C(23)	1.004(2)	0.925 5(7)	0.297 8(9)	C(405)	0.594(2)	0.324(1)	0.174(1)
C(24)	0.922(2)	0.944 6(8)	0.360(1)	C(406)	0.574(2)	0.405(1)	0.178(1)
C(25)	0.848(2)	0.888 6(8)	0.403 7(8)				

carried out a single-crystal X-ray crystallographic structure determination of a representative example, $[MnBr_2L^1]$, crystallised from acetone–benzene as a monobenzene solvate. The complex $[MnBr_2L^1]$ displays distorted trigonal-bipyramidal geometry around the metal centre, the trigonal plane comprising the pyridyl nitrogen N(21) of the tridentate ligand and the two bromines, leaving the two imino nitrogen atoms, N(10) and N(30), disposed above and below the plane as the apical donor atoms. Only a few trigonal-bipyramidal manganese(II) complexes have been characterised structurally *e.g.* $[MnBr_2(dmu)_3]$,[22] $[MnCl_2(mim)_3]$,[23] $[MnCl_2(L')]$,[24] and $[MnBr\{N(CH_2CH_2NMe_2)_3\}]^+$,[25] the last two also containing tridentate ligands {dmu = *N*,*N*′-dimethylurea, mim = 2-methylimidazole, L′ = 1,2,3,4-tetrahydro-2-[2-methyl-3-(2′-pyridyl)pyridylimino]-4-oxoquinazoline}. There is no evidence of polymerisation in $[MnBr_2L^1]$, unlike $[MnCl_2L^6]$ which in the solid state displays pentagonal-bipyramidal geometry by chlorine bridging[13] or $[Mn\{N(CH_2CH_2NH_2)_3\}X]^+$ (X = NCS or NCO) which are weakly associated dimers *via* hydrogen bonding.[20]

The trigonal plane in $[MnBr_2L^1]$ has all three angles close to 120° [Br(1)–Mn–Br(2) 121.3, Br(1)–Mn–N(21) 119.8, and Br(2)–Mn–N(21) 118.8°] but strain induced by the tridentate ligand considerably reduces the axial N(10)–Mn–N(30) angle to 142.8°, a similar feature also being apparent in $[MnCl_2L']$[24] where the axial O–Mn–N angle is 139.9°. The Mn–Br bond

Table 3. Final intramolecular bond distances (pm) and angles (°) in $[MnBr_2L^1]\cdot C_6H_6$

Mn–Br(1)	246.5(2)	N(21)–C(26)	133(1)	C(13)–C(14)	136(3)	C(30)–C(301)	153(2)
Mn–Br(2)	248.9(2)	N(30)–C(30)	128(1)	C(14)–C(15)	135(3)	C(31)–C(32)	137(2)
Mn–N(10)	226(1)	N(30)–C(31)	147(1)	C(15)–C(16)	136(2)	C(31)–C(36)	137(2)
Mn–N(21)	217.7(9)	C(10)–C(22)	148(2)	C(22)–C(23)	141(2)	C(32)–C(33)	138(2)
Mn–N(30)	225(1)	C(10)–C(101)	148(2)	C(23)–C(24)	134(2)	C(33)–C(34)	137(2)
N(10)–C(10)	128(2)	C(11)–C(12)	137(2)	C(24)–C(25)	138(2)	C(34)–C(35)	137(2)
N(10)–C(11)	144(2)	C(11)–C(16)	136(2)	C(25)–C(26)	140(2)	C(35)–C(36)	140(2)
N(21)–C(22)	136(2)	C(12)–C(13)	141(2)	C(26)–C(30)	146(2)		
Br(1)–Mn–Br(2)	121.26(9)	N(10)–C(10)–C(101)	128(2)	Mn–N(21)–C(22)	118.5(9)	C(10)–C(22)–C(23)	125(2)
Br(1)–Mn–N(10)	97.1(3)	C(22)–C(10)–C(101)	116(1)	Mn–N(21)–C(26)	120.9(9)	C(22)–C(23)–C(24)	119(2)
Br(1)–Mn–N(21)	119.8(3)	N(10)–C(11)–C(12)	117(1)	C(22)–N(21)–C(26)	121(1)	C(23)–C(24)–C(25)	122(1)
Br(1)–Mn–N(30)	100.0(3)	N(10)–C(11)–C(16)	123(2)	Mn–N(30)–C(30)	118.8(9)	C(24)–C(25)–C(26)	117(1)
Br(2)–Mn–N(10)	102.3(3)	C(12)–C(11)–C(16)	120(2)	Mn–N(30)–C(31)	121.4(7)	N(21)–C(26)–C(25)	122(1)
Br(2)–Mn–N(21)	118.8(3)	C(11)–C(12)–C(13)	119(2)	C(30)–N(30)–C(31)	120(1)	N(21)–C(26)–C(30)	113(1)
Br(2)–Mn–N(30)	96.6(3)	C(12)–C(13)–C(14)	121(2)	C(25)–C(26)–C(30)	125(1)	C(32)–C(31)–C(36)	119(1)
N(10)–Mn–N(21)	72.2(4)	C(13)–C(14)–C(15)	118(2)	N(30)–C(30)–C(26)	116(1)	C(31)–C(32)–C(33)	121(1)
N(10)–Mn–N(30)	142.8(4)	C(14)–C(15)–C(16)	124(2)	N(30)–C(30)–C(301)	126(1)	C(32)–C(33)–C(34)	119(1)
N(21)–Mn–N(30)	70.6(4)	C(11)–C(16)–C(15)	119(2)	C(26)–C(30)–C(301)	118(1)	C(33)–C(34)–C(35)	121(2)
Mn–N(10)–C(10)	118(1)	N(21)–C(22)–C(10)	115(1)	N(30)–C(31)–C(32)	120(1)	C(34)–C(35)–C(36)	119(1)
Mn–N(10)–C(11)	121.1(7)	C(10)–N(10)–C(11)	119(1)	N(30)–C(31)–C(36)	120(1)	C(31)–C(36)–C(35)	120(1)
N(10)–C(10)–C(22)	116(1)			N(21)–C(22)–C(23)	120(2)		

Table 4. Final fractional atomic co-ordinates for $[ZnCl_2L^1]\cdot 1.5MeCN$

Atom	*x*	*y*	*z*	Atom	*x*	*y*	*z*
Zn(1)	0.291 4(1)	0.964 6(1)	0.737 0(1)	Zn(2)	0.381 2(1)	0.465 4(1)	0.327 5(1)
Cl(1)	0.182 1(3)	1.064 9(2)	0.800 2(1)	Cl(3)	0.321 4(3)	0.313 3(2)	0.272 9(1)
Cl(2)	0.444 1(3)	1.044 6(2)	0.678 6(1)	Cl(4)	0.217 3(3)	0.522 2(2)	0.385 8(1)
N(1)	0.461 0(8)	0.904 1(6)	0.808 4(3)	N(4)	0.339 0(8)	0.582 1(6)	0.252 7(3)
N(2)	0.244 2(8)	0.799 0(5)	0.736 9(3)	N(5)	0.582 1(8)	0.560 4(6)	0.329 6(3)
N(3)	0.085 3(9)	0.928 7(6)	0.667 3(3)	N(6)	0.550 4(8)	0.403 1(6)	0.402 3(3)
C(1)	0.124 3(10)	0.754 8(7)	0.698 5(4)	C(1′)	0.586 6(10)	0.641 2(7)	0.290 5(4)
C(2)	0.082 7(11)	0.644 9(8)	0.701 2(4)	C(2′)	0.719 1(11)	0.709 0(8)	0.293 2(4)
C(3)	0.165 4(11)	0.587 4(8)	0.742 5(4)	C(3′)	0.839 2(12)	0.691 8(8)	0.336 0(5)
C(4)	0.287 5(11)	0.632 4(7)	0.780 3(4)	C(4′)	0.836 6(11)	0.609 6(7)	0.375 9(4)
C(5)	0.324 9(10)	0.742 0(7)	0.777 3(4)	C(5′)	0.700 9(11)	0.544 7(7)	0.370 4(4)
C(6)	0.450 5(11)	0.803 7(8)	0.817 1(4)	C(6′)	0.448 9(11)	0.648 8(8)	0.246 9(4)
C(7)	0.545 8(12)	0.747 2(8)	0.864 9(5)	C(7′)	0.450 4(13)	0.732 5(8)	0.200 6(5)
C(8)	0.573 4(11)	0.970 3(7)	0.846 3(4)	C(8′)	0.195 6(11)	0.581 2(7)	0.213 2(4)
C(9)	0.542 7(13)	1.010 0(8)	0.900 5(5)	C(9′)	0.103 7(12)	0.663 2(8)	0.220 2(5)
C(10)	0.648 6(14)	1.078 0(10)	0.936 3(6)	C(10′)	−0.035 0(13)	0.663 1(9)	0.181 2(5)
C(11)	0.781 8(15)	1.108 1(10)	0.916 3(6)	C(11′)	−0.076 8(13)	0.584 5(9)	0.138 5(5)
C(12)	0.809 5(14)	1.072 6(9)	0.862 2(5)	C(12′)	0.015 9(13)	0.501 7(10)	0.132 9(5)
C(13)	0.704 5(12)	1.004 5(8)	0.824 3(5)	C(13′)	0.153 7(12)	0.503 9(8)	0.170 6(5)
C(14)	0.040 7(11)	0.830 1(8)	0.658 7(4)	C(14′)	0.677 9(11)	0.451 3(7)	0.409 7(4)
C(15)	−0.091 7(11)	0.785 2(8)	0.613 6(4)	C(15′)	0.809 0(12)	0.421 5(9)	0.454 7(5)
C(16)	0.007 2(11)	1.010 1(7)	0.633 7(4)	C(16′)	0.511 8(10)	0.312 6(7)	0.438 0(4)
C(17)	−0.120 4(12)	1.043 5(8)	0.651 8(5)	C(17′)	0.483 2(12)	0.330 8(9)	0.494 9(5)
C(18)	−0.196 4(13)	1.123 0(9)	0.618 4(5)	C(18′)	0.439 7(13)	0.243 9(9)	0.530 3(6)
C(19)	−0.145 7(13)	1.159 9(9)	0.567 9(5)	C(19′)	0.426 4(12)	0.143 5(9)	0.504 3(5)
C(20)	−0.018 2(14)	1.128 6(9)	0.551 3(5)	C(20′)	0.460 0(11)	0.128 6(8)	0.446 8(4)
C(21)	0.062 3(13)	1.051 8(8)	0.584 8(5)	C(21′)	0.499 6(11)	0.210 7(8)	0.413 2(5)
				C(2′1)	0.121 9(16)	0.803 3(10)	0.892 2(6)
				C(2′2)	−0.012 8(14)	0.808 4(10)	0.850 0(6)
				N(7)	0.230 2(15)	0.795 0(12)	0.922 6(5)
				C(3′1)	0.414 2(23)	0.557 1(14)	0.062 2(9)
				C(3′2)	0.279 2(22)	0.583 2(13)	0.022 6(8)
				N(8)	0.511 7(18)	0.531 2(14)	0.093 5(8)
				C(4′1)	0.185 6(23)	0.246 5(17)	−0.007 1(8)
				C(4′2)	0.253 5(25)	0.176 3(17)	−0.041 5(8)
				N(9)	0.139 2(21)	0.307 2(14)	0.018 9(8)

lengths in $[MnBr_2L^1]$, mean 247.7 pm, are shorter than those found in $[MnBr_2(dmu)_3]$, mean 256.3 pm,[22] but similar to those in both $[MnBr\{N(CH_2CH_2NMe_2)_3\}]^+$,[25] 249.1 pm, and $[MnBr_3(OPPhMe_2)]^-$, mean 248.0 pm.[26]

The ligand L^1 binds as a tridentate ligand, all nitrogen and carbon atoms of the ligand skeleton being planar with only the two phenyl rings being twisted out of the co-ordination plane. The two axial Mn–N(imino) bonds are essentially identical (225, 226 pm) in length but the central pyridyl nitrogen forms a significantly shorter Mn–N bond of 217.7 pm as a result of the

Table 5. Final intramolecular bond distances (pm) and angles (°) in $[ZnCl_2L^1]\cdot 1.5MeCN$

Molecule 1				Molecule 2			
Zn(1)–Cl(1)	225.1(3)	C(5)–C(6)	149(1)	Zn(2)–Cl(3)	223.8(3)	C(6′)–C(7′)	149(1)
Zn(1)–Cl(2)	222.2(3)	C(6)–C(7)	149(1)	Zn(2)–Cl(4)	224.6(3)	C(4′)–C(5′)	140(1)
Zn(1)–N(1)	222.6(7)	C(4)–C(5)	140(1)	Zn(2)–N(4)	225.1(8)	C(3′)–C(4′)	138(1)
Zn(1)–N(2)	209.5(7)	C(3)–C(4)	136(1)	Zn(2)–N(5)	208.1(7)	C(2′)–C(3′)	137(1)
Zn(1)–N(3)	225.0(7)	C(2)–C(3)	135(1)	Zn(2)–N(6)	228.2(7)	C(1′)–C(2′)	140(1)
N(1)–C(6)	128(1)	C(1)–C(2)	141(1)	N(4)–C(6′)	127(1)	C(1′)–C(6′)	147(1)
N(1)–C(8)	143(1)	C(1)–C(14)	148(1)	N(4)–C(8′)	145(1)	C(14′)–C(15′)	151(1)
N(2)–C(1)	135(1)	C(14)–C(15)	151(1)	N(5)–C(1′)	135(1)	C(16′)–C(17′)	135(1)
N(2)–C(5)	133(1)			N(5)–C(5′)	133(1)	C(16′)–C(21′)	138(1)
N(3)–C(14)	128(1)			N(6)–C(14′)	124(1)	C(17′)–C(18′)	142(2)
N(3)–C(16)	144(1)			N(6)–C(16′)	145(1)		
				C(5′)–C(14′)	150(1)		
Cl(1)–Zn(1)–Cl(2)	119.0(2)	C(10)–C(11)–C(12)	120.4(11)	Cl(3)–Zn(2)–Cl(4)	119.1(1)	N(5)–Zn(2)–N(6)	73.2(3)
Cl(1)–Zn(1)–N(1)	95.8(2)	C(11)–C(12)–C(13)	121.9(12)	Cl(3)–Zn(2)–N(4)	99.1(2)	Zn(2)–N(4)–C(6′)	115.8(6)
Cl(1)–Zn(1)–N(2)	117.8(2)	C(8)–C(13)–C(12)	117.1(10)	Cl(3)–Zn(2)–N(5)	124.8(2)	Zn(2)–N(4)–C(8′)	122.3(6)
Cl(1)–Zn(1)–N(3)	96.8(2)	N(2)–C(5)–C(6)	115.1(8)	Cl(3)–Zn(2)–N(6)	98.1(2)	C(6′)–N(4)–C(8′)	121.8(8)
Cl(2)–Zn(1)–N(1)	100.2(2)	N(2)–C(5)–C(4)	119.7(8)	Cl(4)–Zn(2)–N(4)	97.7(2)	Zn(2)–N(5)–C(1′)	118.6(5)
Cl(2)–Zn(1)–N(2)	123.2(2)	C(6)–C(5)–C(4)	125.2(8)	Cl(4)–Zn(2)–N(5)	116.1(2)	Zn(2)–N(5)–C(5′)	120.5(6)
Cl(2)–Zn(1)–N(3)	99.3(2)	C(5)–C(4)–C(3)	118.7(9)	Cl(4)–Zn(2)–N(6)	98.1(2)	C(1′)–N(5)–C(5′)	120.8(7)
N(1)–Zn(1)–N(2)	73.7(3)	C(4)–C(3)–C(2)	121.9(9)	N(4)–Zn(2)–N(5)	74.0(3)	Zn(2)–N(6)–C(14′)	115.3(6)
N(1)–Zn(1)–N(3)	148.0(3)	C(3)–C(2)–C(1)	118.2(8)	N(4)–Zn(2)–N(6)	147.1(3)	Zn(2)–N(6)–C(16′)	122.1(5)
N(2)–Zn(1)–N(3)	74.4(3)	N(2)–C(1)–C(2)	119.4(8)	C(14′)–N(6)–C(16′)	122.6(8)	C(2′)–C(3′)–C(4′)	122.7(9)
Zn(1)–N(1)–C(6)	116.8(6)	N(2)–C(1)–C(14)	115.5(7)	N(4)–C(16′)–C(1′)	115.9(8)	C(3′)–C(4′)–C(5′)	115.5(9)
Zn(1)–N(1)–C(8)	124.2(6)	C(2)–C(1)–C(14)	125.0(8)	N(4)–C(6′)–C(7′)	126.2(9)	N(5)–C(5′)–C(4′)	122.9(8)
C(6)–N(1)–C(8)	118.9(8)	N(3)–C(14)–C(1)	116.2(8)	C(1′)–C(6′)–C(7′)	117.9(8)	N(5)–C(5′)–C(14′)	114.2(8)
Zn(1)–N(2)–C(5)	119.3(5)	N(3)–C(14)–C(15)	125.8(9)	N(4)–C(8′)–C(9′)	118.2(8)	C(4′)–C(5′)–C(14′)	122.9(8)
Zn(1)–N(2)–C(1)	118.4(6)	C(1)–C(14)–C(15)	118.0(8)	N(4)–C(8′)–C(13′)	120.9(9)	N(6)–C(14′)–C(5′)	116.8(8)
C(1)–N(2)–C(5)	112.1(7)	N(3)–C(16)–C(17)	119.2(9)	N(5)–C(1′)–C(6′)	115.6(8)	N(6)–C(14′)–C(15′)	124.5(9)
Zn(1)–N(3)–C(14)	115.5(6)	N(3)–C(16)–C(21)	119.6(9)	N(5)–C(1′)–C(2′)	119.3(8)	C(5′)–C(14′)–C(15′)	118.7(8)
Zn(1)–N(3)–C(16)	123.3(5)	C(5)–C(6)–C(7)	119.1(8)	C(6′)–C(1′)–C(2′)	125.1(9)	N(6)–C(16′)–C(17′)	118.6(8)
C(14)–N(3)–C(16)	121.2(7)	N(1)–C(8)–C(9)	119.9(9)	C(1′)–C(2′)–C(3′)	118.7(9)	N(6)–C(16′)–C(21′)	120.3(8)
N(1)–C(6)–C(5)	114.9(8)	N(1)–C(8)–C(13)	118.9(9)				
N(1)–C(6)–C(7)	125.8(8)						
Solvent molecules							
N(7)–C(2′1)	112(2)	C(2′1)–C(2′2)	143(2)				
N(8)–C(3′1)	111(3)	C(3′1)–C(3′2)	146(3)				
N(9)–C(4′1)	110(3)	C(4′1)–C(4′2)	139(3)				
N(7)–C(2′1)–C(2′2)	176(1)	N(8)–C(3′1)–C(3′2)	175(2)				
N(9)–C(4′1)–C(4′2)	175(2)						

Table 6. Infrared, magnetic, and conductivity data

	$[MnCl_2L^1]$	$[MnBr_2L^1]$	$[MnCl_2L^2]$	$[MnBr_2L^2]$
Λ_M (10^{-3} mol dm^{-3}, MeCN, S m^2 mol^{-1})	61.4	42.0	32.4	35.6
$\mu_{eff.}$, room temperature	5.87	5.82	5.80	5.88
I.r. ν(C=N) + py and aryl-ring deformations (cm^{-1})*	1 619s, 1 591s, 1 580s	1 615ms, 1 580s, 1 557 (sh)	1 610ms, 1 580s (br)	1 615m, 1 575s, 1 552 (sh)
I.r. ν(Mn–X) (cm^{-1})	301s, 280m	248s, 229m	299s, 273m	243s, 210m

* Free L^1: 1 635s, 1 595m, and 1 575s cm^{-1}. Free L^2: 1 624s, 1 593s, and 1 568s cm^{-1}.

constrained ligand geometry. This strain is apparent on consideration of the reduced N(10)–Mn–N(21) and N(30)–Mn–N(21) bite angles (*i.e.* the angle subtended between adjacent nitrogen donor atoms and the metal) of 72.2 and 70.6°, respectively. Similar features of a shorter central M–N(py) bond length and reduced mean bite angles within the tridentate ligand have been noted for $[Cu(\eta^2\text{-}NO_3)(NO_3)L^1]$[4] (central Cu–N shorter by 13 pm; mean bite angle 79.6°), $[Ni(\eta^2\text{-}NO_3)(NO_3)L^1]$[2,3] (central Ni–N shorter by 13 pm, mean bite angle 78.2°), and $[Cu(bipy)L^4(FBF_3)]^+$ (central Cu–N shorter by 15 pm and mean bite angle 79.0°).[9] Short M–N(py) distances are also a feature of a wide variety of first-row transition metal–macrocyclic nitrogen-donor ligand complexes studied in recent years by Moore and co-workers.[27] It is interesting that in *cis*-$[Mo(CO)_4L^1]$, the only structurally characterised complex containing an L type ligand displaying bidentate behaviour,[10] the Mo–N(py) distance is slightly *longer* than the Mo–N(imino) distance even though the bite angle of 72.5° is still much reduced from 90°.

The mean N–C (134.5 pm) and C–C (138 pm) distances in the pyridyl ring, the mean C–C (137 pm) distance in the phenyl rings, and the mean C(sp^2)–C(methyl) (150 pm) and C(sp^2)–C(phenyl) (147 pm) distances are unremarkable. The C(10)–N(10) and C(30)–N(30) distances (mean 128 pm) are as expected for C=N azomethine bonds.

Table 7. Bond length (pm) and angle (°) comparisons for $[ZnCl_2L^1]\cdot 1.5MeCN$ and $[ZnCl_2L^6]\cdot H_2O$[28]

	$[ZnCl_2L^1]\cdot 1.5MeCN$ *	$[ZnCl_2L^6]\cdot H_2O$
Zn–Cl	233.8, 224.6	233.3, 224.4
Zn–N(pyridyl)	208.1	206.3
Zn–N(aryl/OH)	225.1, 228.2	223.8, 224.6
Cl–Zn–Cl	119.1	121.2
Cl–Zn–N(pyridyl)	116.1, 124.8	116.6, 122.1
Axial N–Zn–N	147.1	147.3
(pyridyl)N–Zn–N(aryl/OH)	73.2, 74.0	73.2, 74.1

* Molecule 2 of the two independent molecules in the asymmetric unit. Similar comparisons can be made using Molecule 1.

(*b*) *The Structure of* $[ZnCl_2L^1]\cdot 1.5MeCN$.—In order to establish that the later first-row transition-metal and zinc halides probably form a structurally analogous series of five-co-ordinate $[MX_2L^1]$ complexes, we have also determined the structure of $[ZnCl_2L^1]$ obtained as single crystals of the sesquisolvate from acetonitrile solution. The lattice acetonitrile molecules form no close contacts with the distorted trigonal-bipyramidal $[ZnCl_2L^1]$ units, there being two independent molecules of the complex and three solvate molecules in the asymmetric unit. The two independent $[ZnCl_2L^1]$ molecules have closely similar dimensions, *e.g.* Zn–Cl distances of 222.2 and 225.1 *vs.* 223.8 and 224.6 pm and Zn–N distances of 209.5, 222.6, and 225.0 *vs.* 208.1, 225.1, and 228.2 pm, the shortest distances involving, as discussed for $[MnBr_2L^1]$, the pyridyl nitrogens. The trigonal angles of the two molecules are all close to 120° and in both molecules increase in the sequence Cl(1) or (4)–Zn–N(py) < Cl–Zn–Cl < Cl(2) or (3)–Zn–N(py) (117.8, 119.0, and 123.2 for molecule 1 and 116.1, 119.1, and 124.8° for molecule 2). The axial (imino)N–Zn–N(imino) angles in both molecules are very similar and much reduced from 180° (148.0 and 147.1°, respectively) as a result of the strain induced by the planar tridentate ligand L^1, as discussed earlier for $[MnBr_2L^1]$. All (imino)N–Zn–N(py) bite angles fall in the range 73.2—74.4°, again much reduced from 90° due to tridentate ligand strain. The axial (imino)N–Mn–N(imino) angle of 142.8° and the (imino)N–Mn–N(py) bite angles of 70.6 and 72.2° in $[MnBr_2L^1]$ are more reduced from 180 and 90°, respectively, than found in the independent $[ZnCl_2L^1]$ molecules as a result of the planar tridentate L^1 being co-ordinated to the larger $MnBr_2$ moiety.

The mean dimensions of $[ZnCl_2L^1]\cdot 1.5MeCN$ can be compared with those reported[28] for the dioxime complex $[ZnCl_2L^6]\cdot H_2O$ which also involves distorted trigonal-bipyramidal co-ordination for zinc derived from two equatorial chlorines and a planar tridentate ligand. In this example, however, the two axial nitrogen-donor atoms are oxime nitrogens rather than imine nitrogens. The close similarities (*e.g.* Zn–Cl, Zn–N distances, shorter pyridyl N–Zn distances, and the effect of tridentate ligand strain on the axial N–Zn–N angle) which are evident are summarised in Table 7. The replacement of the phenyl groups of $[ZnCl_2L^1]$ by hydroxyl groups in $[ZnCl_2L^6]$ causes slight shortening of the Zn–N bonds and opening of the Cl–Zn–Cl angle.

(*c*) $[MnL^1{}_2]^{2+}$ *and* $[MnL^2{}_2]^{2+}$ *Complexes*.—These two cations have been isolated as perchlorate salts and the physical data obtained point to the cations being octahedral with two meridionally disposed tridentate ligands. This structural type has been proposed for $[MnL^6{}_2]X_2$ (X = Cl, Br, I, NO_3, NCS, or NCSe)[12] and established by a crystal-structure determination for $[NiL^3{}_2][BF_4]_2$, in which four imine nitrogen-donor atoms form the equatorial plane with two shorter Ni–N(pyridyl) bonds axial.[8]

Molar conductivities of $[MnL^1{}_2][ClO_4]_2$ and $[MnL^2{}_2][ClO_4]_2$ as 10^{-3} mol dm^{-3} solutions in acetonitrile at 25 °C were 298 and 246 S m^2 mol^{-1}, respectively, in line with expectations for 2:1 electrolytes in this solvent.[29] Apart from bands of co-ordinated ligands, the i.r. spectra show strong bands at 1 065—1 080 (br) and 620 cm^{-1}, assigned to the ν(ClO) and δ(OClO) vibrations of the perchlorate anions. Solid-state magnetic moments, measured at 25 °C by the Gouy method, of 5.85 and 5.95 for the $[MnL^1{}_2]^{2+}$ and $[MnL^2{}_2]^{2+}$ complexes, respectively, also indicate the presence of high-spin octahedral manganese(II). The *X*-band e.p.r. spectra of the two complexes show prominent fine-structure splittings between 1 400 and 5 400 G but no resolved hyperfine structure from ^{55}Mn. The fine structure is very similar to that observed for $[MnL^6{}_2]X_2$ (X = Br or ClO_4),[13] and for the hydridotris(1-pyrazolyl)-borato complex $[Mn\{HB(pz)_3\}_2]$ (see Figure 4 of ref. 13). The e.p.r. spectra are thus consistent with the presence of monomeric trigonally distorted octahedral manganese(II) with zero-field splitting of 0.2 cm^{-1} or greater.[21].

Attempts to prepare the bis(ligand) complexes as the chloride or bromide salts by treating the metal halides with 2 equivalents of the ligands in ethanol were unsuccessful, mixed products being obtained with analyses between $[MnX_2L]$ and $[MnL_2]X_2$. These were not studied further. Conversely, reactions between equimolar amounts of $Mn(ClO_4)_2\cdot 6H_2O$ and L^1 or L^2 merely gave reduced yields of $[MnL_2][ClO_4]_2$. Thus, the type of anion present is significant in determining the nature of the product.

Acknowledgements

We thank the National Science Foundation for the purchase of a Microvax computer and CAD-4 diffractometer at Purdue University (Grant No. CHE-8615556).

References

1 E. C. Alyea and P. H. Merrell, *Synth. React. Inorg. Metal-Org. Chem.*, 1974, **4**, 535.
2 E. C. Alyea, G. Ferguson, R. J. Restivo, and P. H. Merrell, *J. Chem. Soc., Chem. Commun.*, 1975, 269.
3 E. C. Alyea, G. Ferguson, and R. J. Restivo, *Inorg. Chem.*, 1975, **14**, 2491.
4 G. Ferguson and R. J. Restivo, *J. Chem. Soc., Dalton Trans.*, 1976, 518.
5 E. C. Alyea and P. H. Merrell, *Inorg. Chim. Acta*, 1978, **28**, 91.
6 P. H. Merrell, E. C. Alyea, and L. Ecott, *Inorg. Chim. Acta*, 1982, **59**, 25.
7 E. C. Alyea, *Inorg. Chim. Acta*, 1983, **76**, L239.
8 A. J. Blake, A. J. Lavery, T. I. Hyde, and M. Schröder, *J. Chem. Soc., Dalton Trans.*, 1989, 965.
9 E. C. Alyea, G. Ferguson, M. Nahuis, and B. L. Ruhl, *J. Cryst. Spect. Res.*, 1985, **15**, 523.
10 S. Lu and J. Selbin, *Inorg. Chim. Acta*, 1987, **134**, 229.
11 J. M. Albon, D. A. Edwards, and P. J. Moore, *Inorg. Chim. Acta*, 1989, **159**, 19.
12 M. Mohan and M. Kumar, *Transition Met. Chem. (Weinheim, Ger.)*, 1985, **10**, 255.
13 B. C. Unni Nair, J. E. Sheats, R. Ponteciello, D. Van Engen, V. Petrouleas, and G. C. Dismukes, *Inorg. Chem.*, 1989, **28**, 1582.
14 N. Walker and D. Stuart, *Acta Crystallogr., Sect. A*, 1983, **39**, 158.
15 D. T. Cromer, 'International Tables for *X*-Ray Crystallography,' Kynoch Press, Birmingham, 1974, vol. 4, table 2.3.1; D. T. Cromer and J. T. Waber, *ibid.*, table 2.2B.
16 D. T. Cromer and J. B. Mann, *Acta Crystallogr., Sect. A*, 1968, **24**, 321.
17 R. F. Stewart, E. R. Davidson, and W. T. Simpson, *J. Chem. Phys.*, 1965, **42**, 3175.
18 D. T. Cromer and D. J. Liberman, *J. Chem. Phys.*, 1970, **53**, 1891.
19 D. Bryson and R. H. Nuttall, *Spectrochim. Acta, Part A*, 1970, **26**, 2275.
20 E. J. Laskowski and D. N. Hendrickson, *Inorg. Chem.*, 1978, **17**, 457.

21 R. D. Dowsing and J. F. Gibson, *J. Chem. Phys.*, 1969, **50**, 294; R. D. Dowsing, J. F. Gibson, D. M. Goodgame, M. Goodgame, and P. J. Hayward, *Nature (London)*, 1968, **219**, 1037.
22 J. Delaunay and R. P. Hugel, *Inorg. Chem.*, 1986, **25**, 3957.
23 F. L. Phillips, F. M. Shreeve, and A. C. Skapski, *Acta Crystallogr., Sect. B*, 1976, **32**, 687.
24 C. Pelizzi and G. Pelizzi, *Acta Crystallogr., Sect. B*, 1974, **30**, 2421.
25 M. Di Vaira and P. L. Orioli, *Acta Crystallogr., Sect. B*, 1968, **24**, 1269.
26 B. Beagley, C. G. Benson, G. A. Gott, C. A. McAuliffe, R. G. Pritchard, and S. P. Tanner, *J. Chem. Soc., Dalton Trans.*, 1988, 2261.
27 N. W. Alcock, P. Moore, C. J. Reader, and S. M. Roe, *J. Chem. Soc., Dalton Trans.*, 1988, 2959 and refs. therein.
28 G. A. Nicholson, J. L. Petersen, and B. J. McCormick, *Inorg. Chem.*, 1982, **21**, 3274.
29 W. J. Geary, *Coord. Chem. Rev.*, 1971, **7**, 81.

Received 14*th May* 1990; *Paper* 0/02141E